

Interstellar Dust

M. Compiègne

Canadian Institute for Theoretical Astrophysics, University of Toronto, 60 St. George Street, Toronto, ON M5S 3H8, Canada

Abstract. Dust is a key component of the Universe, especially regarding galaxy evolution, playing an essential role for both the physics and chemistry of the interstellar medium. In this paper, we give a brief review of interstellar dust. We describe the main dust observables and how they allow us to constrain dust properties. We discuss the dust life-cycle and the dust evolution in the ISM. We also present a physical dust model, DustEM.

1. Introduction

Dust is a fundamentally important component of the Universe. The presence of sub-micron size particles in the interstellar medium (ISM) was definitely evidenced by Trumpler (1930) through the reddening of starlight. These particles were first considered as a nuisance for the estimate of stellar distances. Since that time and through the study of the ISM, there was growing evidence that dust is an essential component in the life of the ISM and thus, for the evolution of galaxies. The ubiquity of dust in any phase of the ISM (and in other galaxies) was truly revealed by the first infrared surveys, especially the Infrared Astronomical Satellite (IRAS). Dust is now widely used to trace ISM physical conditions (e.g. Bernard et al. 2010) and structure (e.g. Miville-Deschênes et al. 2010). It has also been detected in the early universe, in quasars at redshift $z \gtrsim 6$ (e.g. Beelen et al. 2006).

Despite the fact that it represents a small mass fraction of the ISM ($\sim 1\%$) dust plays a crucial role for its physics and chemistry. Among the most important impacts of dust onto the gas phase, we have (i) the photoelectric effect that is the main heating process of the diffuse gas in the ISM, (ii) the catalysis of H_2 formation on the dust surface, otherwise very inefficient in gas phase under ISM conditions because it involves a three-body reaction and (iii) the screening of photo-dissociating photons that allows for the survival of molecules in the ISM. Regarding the role of dust for the thermal balance, it does not only contribute by heating the gas through photoelectric effect: 30% or more of the UV-visible photons emitted by stars are absorbed by the dust that re-emits the absorbed energy in form of an infrared-millimeter (IR-mm) thermal radiation for which the ISM is transparent. For the same reason, dust shapes the appearance of a galaxy at both UV-visible and IR-mm wavelengths. Dust couples the magnetic field to the gas phase in the dense low ionized medium while it is responsible for such low ionization state of the gas through radiation field screening. Consequently, it plays an essential role in the last steps of core collapse during star formation. Dust can also dynamically

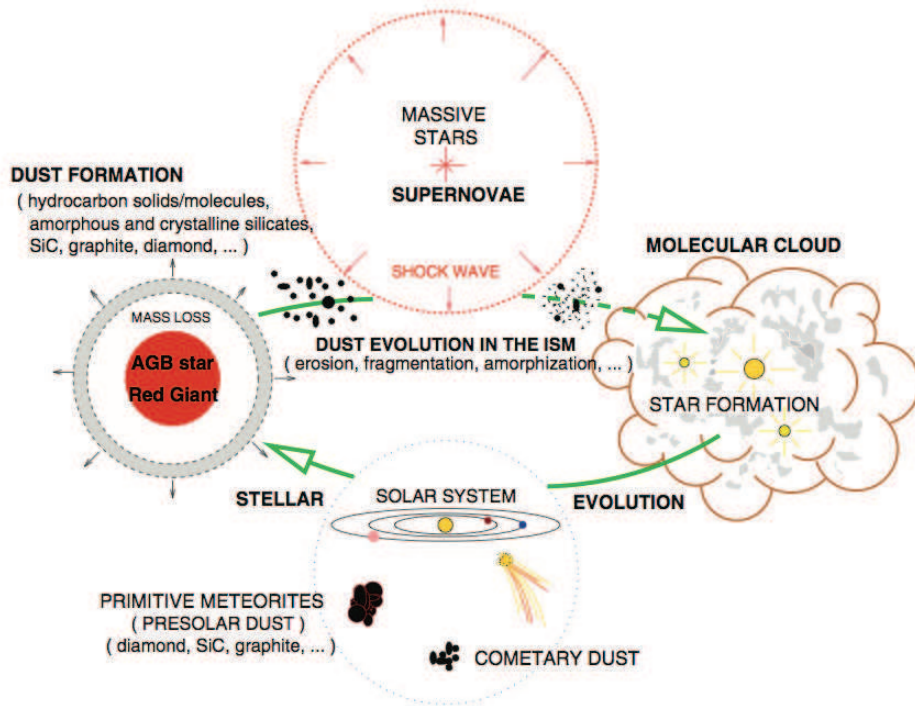


Figure 1. Schematic view of the dust evolution cycle driven by stellar \leftrightarrow ISM matter cycle (from Jones 2004). Note that the dust life-cycle also comprises other short-cuts and sub-loops (e.g. diffuse \leftrightarrow dense ISM cycling, see § 6).

couple the radiation field to the gas since it is more subject to radiation pressure and can drag the gas.

It is now well established that dust properties evolve depending on the physical conditions of the ISM. Fig. 1 shows a schematic view of dust evolution driven by the stellar \leftrightarrow ISM matter cycle. There is an interplay between dust and the rest of the ISM since the evolution of the ISM physical properties causes an evolution of the dust properties and subsequently an evolution of the dust impact on the ISM. It is necessary to characterize the physical processes responsible for dust evolution to be able to quantify the dust impact throughout the ISM life-cycle. Assuming some dust properties, the dust emission is widely used to estimate crucial quantities like cloud masses or star forming activity. However, to derive these quantities properly, one would need to take into account the evolution of dust properties, how they affect its emission and how it reflects the ISM properties. Here again, to characterize the dust evolution processes is of prime importance.

Dust study is a very broad topic including astronomical observations from the X-ray to the millimeter range as well as theoretical and laboratory study of the physics and the chemistry of ISM dust analogs (from large molecules to bulk solid). The present paper does not intend to give an exhaustive review about dust. Moreover, it focuses on interstellar dust that, although being linked by its evolution to circumstellar and protoplanetary dust, has quite different properties (see for example table 2 of Jones 2009). For more information, the reader can refer to numerous other reviews (e.g.

Boulanger et al. 2000; Draine 2003, 2004), books and dedicated conference proceedings (e.g. Whittet 2003; Kruegel, E. 2003; Henning et al. 2009; Boulanger et al. 2009). An historical view of dust study can be found in Li & Greenberg (2003) and Li (2005).

In this paper, we first list the dust observables in section 2 and further detail the depletion (§ 3), extinction (§ 4) and thermal emission (§ 5). In section 6, we discuss the dust life-cycle and evolution. We address dust modeling, focusing on the *DustEM* model in section 7. Concluding remarks are given in section 8.

2. Dust Observables

There are numerous direct and indirect observables that can bring constraints on interstellar dust properties. Dwek (2005) gave a list of these observables :

- the extinction, obscuration, and reddening of starlight;
- the IR emission from circumstellar shells and different parts of the ISM (diffuse H I, H II regions, PDRs, and molecular clouds, X-ray emitting plasma);
- the elemental depletion pattern and interstellar abundances;
- the extended red emission (ERE) seen in various nebulae;
- the presence of X-ray, UV, and visual halos around time-variable sources (X-ray binaries, novae, and supernovae);
- the presence of fine structure in the X-ray absorption edges in the spectra of X-ray sources;
- the reflection and polarization of starlight;
- the microwave emission, presumably from spinning dust;
- the presence of interstellar dust and isotopic anomalies in meteorites and the solar system; and
- the production of photo electrons required to heat neutral photo dissociation regions (PDRs).

Even if related to the emission/extinction item, we can add to that list (i) the diffuse interstellar bands (DIBs) seen in the optical/near-IR extinction that were first detected 90 years ago and (ii) the blue luminescence. Identification of the DIB carriers is one of the most challenging problem in the field of dust study since about 400 such bands are observed while none has yet been identified. It demonstrates the great importance of laboratory measurements to characterize more and more ISM dust candidates (in that case, very large molecules).

These observational constraints span a broad range of environments and then various dust properties. Among these observables, the extinction curve, the IR-mm thermal emission and the depletion are the most often used to draw a picture of the average dust properties and how they evolve regarding the ISM properties. We describe these observables in the following sections.

3. Depletion

In the ISM, most of the elements heavier than He are at least partially depleted in the solid phase. As a consequence, the dust to gas mass ratio is correlated to the metallicity (see Draine et al. 2007, for nearby galaxies). The solid phase abundance of an element can be estimated by comparing its abundance in the gas phase with respect to its overall abundance in the ISM that is estimated by measuring its abundance in stellar atmospheres where no solid matter can subsist. Following Jones (2000), we can separate the dust elemental constituents in four categories regarding their abundance in the solid phase: (i) the primary elements, C and O, (ii) the secondary elements, Mg, Si and Fe, (iii) the minority elements, Na, Al, Ca and Ni and (iv) the trace elements, K, Ti, Cr, Mn, Co.

Most current dust models only take into account the primary and secondary elements. Table 1 lists the measured abundance and the inferred dust abundance for these elements. The solar abundances are from Asplund et al. (2009) while the F, G stars abundances are from Sofia & Meyer (2001). The gas phase abundances are from Dwek et al. (1997) for carbon and from Meyer et al. (1998) for oxygen. The Dwek et al. (1997) value for the carbon gas phase abundance is lower than some other measurements (e.g. 140 ± 20 ppm from Cardelli et al. 1996) but is in good agreement with more recent estimates by Sofia & Parvathi (2009). The gas abundances were measured toward diffuse lines of sight so that these abundances rely on refractory dust material (no ices, see § 4).

One should note that there might not be any stellar standard that well represents the overall ISM abundances because the processes of sedimentation and/or ambipolar diffusion during stellar formation could lower the heavy elements abundance in stars (Snow 2000). That could especially be true for B stars that were used as probes of interstellar abundances since their composition was thought to be more representative of the current ISM. Indeed, B stars have a lower metallicity regarding the Sun and young (≤ 2 Gyrs) F, G stars that seem to be more representative of the ISM metallicity. Finally, we emphasize that Draine (2009b) argued that, regarding the current uncertainties on elemental abundances and the various assumptions that are made for the dust properties, a model that departs from the measured elemental solid phase abundances by tens of percent should still be considered as viable.

4. Extinction

Fig. 2 shows the averaged extinction curve for the diffuse ISM. Various spectral features allow us to infer the composition and mineralogy of dust. The shape of the extinction curve and its level normalized to the gas mass provide an information on the size distribution and abundances of the dust (see Weingartner & Draine 2001).

The strongest observed dust feature is seen at 2175 \AA and has a remarkably constant position while its width varies from one line of sight to another. The $\pi \rightarrow \pi^*$ electronic excitation of aromatic carbon (sp^2 hybridization) provides the most straightforward explanation for this feature. However, the exact nature of such carbonaceous material remains unclear. About 20-30% of the carbon cosmic abundance is required to reproduce the strength of this feature. The $\sigma \rightarrow \sigma^*$ electronic excitation of aromatic

Table 1. The elemental abundances (see § 3 for references) in unit of $[X/10^6\text{H}]$ (or ppm).

		C	O	Mg	Si	Fe
Total	Sun	269±33	490±60	40±4	32±2	32±3
	F,G stars	358±82	445±156	42.7±17.2	39.9±13.1	27.9±7.7
Gas		75±25	319±14	~0	~0	~0
Dust	Sun	194±41	171±62	40±4	32±2	32±3
	F,G stars	283±86	126±157	42.7±17.2	39.9±13.1	27.9±7.7

carbon produces another bump at 750 \AA whose red wing provides a natural explanation for the non-linear FUV rise ($6 \lesssim 1/\lambda \lesssim 10 \mu\text{m}^{-1}$).

Narrower features at 3.3 and $3.4 \mu\text{m}$ are attributed to the C-H stretching mode in aliphatic (chain like) and aromatic hydrocarbons, respectively. By comparing their observed profile with laboratory measurements, Pendleton & Allamandola (2002) concluded that the hydrocarbons in the diffuse ISM are $\sim 15\%$ aliphatic and $\sim 85\%$ aromatic (see also Dartois & Muñoz-Caro 2007).

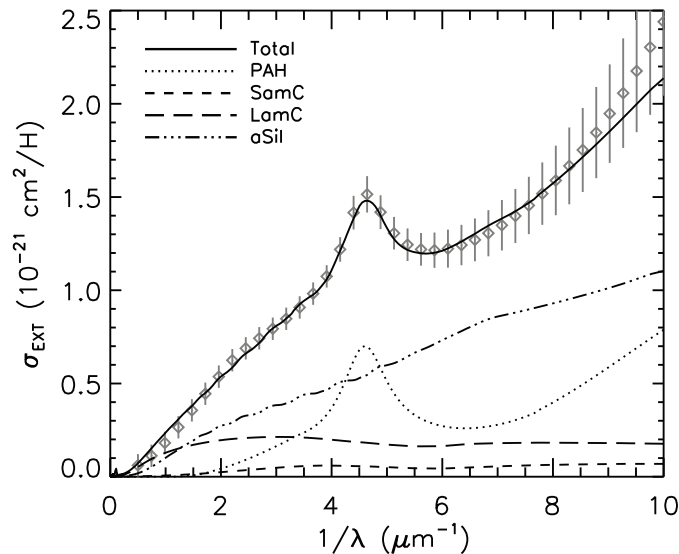


Figure 2. The extinction curve for dust in the diffuse ISM. The grey diamonds show the Fitzpatrick (1999) extinction law for $R_V = 3.1$ and $N_H/E(B - V) = 5.8 \times 10^{21} \text{ H cm}^{-2}$ (Bohlin et al. 1978). The black lines are the DustEM model (see § 7).

Broad bands are seen at 9.7 and $18 \mu\text{m}$ that are attributed to Si-O stretching and O-Si-O bending modes in amorphous silicates, respectively. These bands are strong and require that most of the available Mg, Si, and Fe (if entering the composition of interstellar silicates) are locked in silicates. The exact composition of such silicates is unknown. The absence of fine structure within these broad bands gives a higher limit to the crystallinity. Kemper et al. (2005) gave a limit of $\sim 2\%$ while more recently Li et al. (2007) gave a limit of $\sim 3\text{-}5\%$ taking into account the presence of ice mantles on silicate grains.

Indeed, infrared spectroscopy reveals the presence of extinction features toward dense molecular material ($A_V \gtrsim 3$ on the line of sight, $n_H \gtrsim 10^3 - 10^4 \text{ H cm}^{-3}$) attributed to ices, mainly H_2O , CO_2 and CO . For a review, see Dartois (2005).

Starlight dimmed by dust appears partially polarized. Some grains must then be elongated and aligned with the magnetic field. The decrease of polarization fraction from the visible to the UV (Serkowski 1973) implies that only the bigger grains are efficiently aligned while the smaller grains are not aligned and/or not elongated. On the other hand, the $9.7 \mu\text{m}$ silicate band is polarized while only an upper limit can be estimated for the $3.4 \mu\text{m}$ hydrocarbons band on the same line of sight (e.g. Mason et al. 2007). Although such observations should be pursued, this result may indicate that big carbonaceous (not aligned) and silicate particles (aligned) are at least partially physically separated populations.

In the visible range, the albedo of $\sim 0.4 - 0.6$ and the extinction continuum both require the presence of relatively big grains ($a \sim 0.1 \mu\text{m}$). The high albedo is most likely produced by silicate material that is quite “white” regarding hydrocarbons. The strong increase of extinction from the visible to the vacuum ultraviolet cannot be reproduced without a significant amount of very small particles ($a \lesssim 10 \text{ nm}$). The shape of the extinction curve for a grain with $a \gtrsim 10 \text{ nm}$ depends on its size while it is independent of the size for a smaller grain (in the Rayleigh regime). Consequently, only the abundance of the smaller grains is constrained by the extinction curve, not its size distribution, particularly its lower limit.

5. Emission

Most of the energy absorbed by dust is radiated as IR-mm thermal emission that we describe here. Although most often representing a negligible fraction, heating mechanisms other than the absorption of photons can be efficient in some specific cases like gas-grain collisions in very hot gas of a supernova (SN) remnant¹ (see Dwek & Arendt 1992). Unfortunately, we do not have space in this review to discuss the blue luminescence, the ERE and the near-IR ($\lambda \sim 1 \mu\text{m}$) continuum emission (e.g. Wada et al. 2009; Duley 2009; Flagey et al. 2006) nor the millimeter non-thermal emission of fast spinning grains (e.g. Ysard & Verstraete 2010; Ysard et al. 2010).

Fig. 3 shows the averaged dust spectral energy distribution (SED) for the Diffuse High Galactic Latitude (DHGL) medium ($|b| > 15^\circ$) obtained by Compiègne et al. (2010b) by correlating the IR-mm data with H I-21 cm data.

The bigger grains (BG, $a > 10 \text{ nm}$) are in thermal equilibrium and emit a grey body spectrum in the far-IR. One has to keep in mind that the observed spectrum results from the emission of dust distributed in size and with various compositions that are accordingly distributed in temperature. A physical dust model (see § 7) is then required for a detailed study. However, the far-IR spectrum is often analyzed by fitting a modified blackbody (i.e. grey body) to derive an effective temperature, T_{eff} , and a spectral index β for the emissivity $\sigma_{\text{em}}(\lambda) = \sigma_{\text{abs}}(\lambda) \propto \lambda^{-\beta}$ (e.g. Dupac et al. 2001; Dicker et al. 2009; Bernard et al. 2010). The values derived from DIRBE and FIRAS for the

¹Note that the very hot gas appellation does not apply for $T \sim 10^4 \text{ K}$ as in H II regions where heating by UV photons dominates anyway.

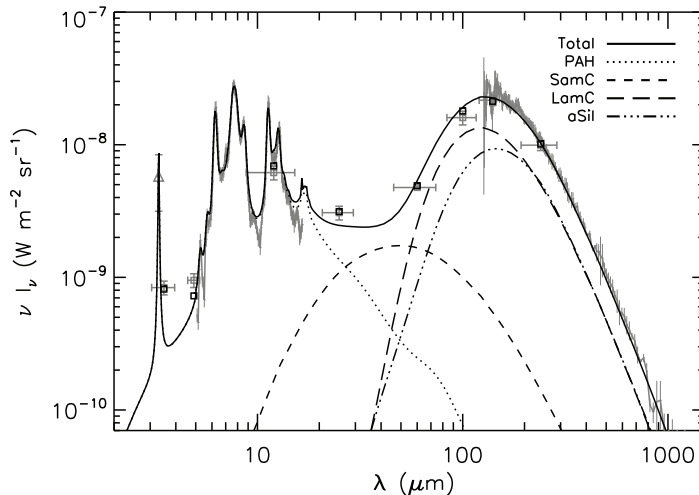


Figure 3. Dust emission for the DHGL medium. Grey symbols and curves indicate the observed emission spectrum (AROME, ISOCAM/CVF, DIRBE, FIRAS) for $N_{\text{H}} = 10^{20} \text{ H cm}^{-2}$ (see Compiègne et al. 2010b, for details). Black lines are the DustEM model output (see § 7) and black squares the modeled DIRBE points.

diffuse interstellar medium are $T_{\text{eff}} = 17.5 \text{ K}$ and $\beta = 2$ (see Boulanger et al. 1996). Taking U to be a scaling factor with respect to the average interstellar exciting radiation field (e.g. the one of Mathis et al. 1983), we can estimate T_{eff} with the formula $T_{\text{eff}} = 17.5 U^{1/(4+\beta)} \text{ K}$. Note that the observed β also varies significantly over the sky (e.g. Dupac et al. 2003; Désert et al. 2008) possibly resulting from the evolution of dust properties and some micro physical effects in amorphous dust grains like the two levels system effect and the disordered charge distribution effect (see Meny et al. 2007). Although they enclose most of the dust mass, the properties of the BGs remain poorly known. New observations currently carried out with Herschel and Planck satellites will bring new insight on those properties.

The IRAS observations revealed the ubiquity of dust mid-IR emission. Such a short wavelength emission requires high temperatures ($T_{\text{eff}} \gtrsim 100 \text{ K}$) that can not be reached by classical BG ($a > 10 \text{ nm}$) at thermal equilibrium unless $U \gtrsim 10^4$. However, a very small grain ($a \sim 1 \text{ nm}$) that has a small heat capacity regarding the energy carried by a single UV-visible photon can reach high temperature in a single photon absorption event. Following such an absorption, it cools down to the fundamental level until the next absorption. For the total spectrum emitted by dust to be computed by accounting for such stochastic heating, one has to derive the probability distribution, dP/dT , of finding a given grain at a temperature in the range $[T, T+dT]$ (see Désert et al. 1986) and then to integrate over T , over all sizes and over all grain types, the emitted spectra weighted by dP/dT . The normalized dP/dT of a stochastically heated particle does not depend on the intensity of the exciting radiation field (i.e. photon absorption rate) as long as the particle undergoes single photon events (i.e. cools down to the fundamental level before a new absorption). It rather depends on the average energy of the absorbed photons. Consequently, unlike the grains at thermal equilibrium, the spectral shape of the emission of the smallest particles does not depend on the intensity of the exciting

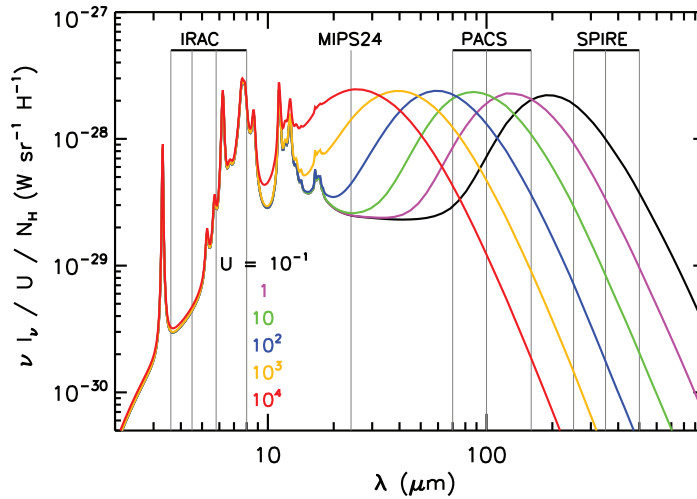


Figure 4. The modeled dust SED per H atom for different scaling factors of the Mathis et al. (1983) exciting radiation field, $U=0.1$ to 10^4 . All spectra have been divided by U to emphasize changes of the SED shape. Also shown are the photometric band positions of Herschel and Spitzer satellites. (Color version online)

radiation field (U) as seen in Fig. 4. Note that for a grain at thermal equilibrium, dP/dT tends toward a Dirac function, $\delta(T - T_{\text{eq}})$.

As a result of stochastic heating, the shape of the near- and mid-IR SED is very sensitive to the size (i.e. the heat capacity) of the very small particles and brings a constraint on its distribution, especially its lower limit. The presence of very small particles ($a \lesssim 1$ nm) is required to explain the observed emission down to $\sim 3 \mu\text{m}$ corresponding to $T \sim 1000$ K. On the other hand, theoretical work has shown that polycyclic aromatic hydrocarbon particles (the smallest ISM dust) smaller than $\sim 3.5 \text{\AA}$ (~ 20 carbon atoms) could not survive in the diffuse ISM due to photolysis (e.g. Allamandola et al. 1989).

Strong emission features at 3.3 , 6.2 , 7.7 , 11.3 and $12.7 \mu\text{m}$ (see Fig. 3) were first observed in NGC7027 by Gillett et al. (1973). Using the Infrared Space Observatory and Spitzer satellites, these features (plus other weaker ones) were detected toward almost every line of sight where dust is present, spanning a broad range of physical conditions. They were first called unidentified infrared bands (UIBs) and were later attributed to the IR fluorescence of UV pumped Polycyclic Aromatic Hydrocarbons (PAH, Duley & Williams 1981; Léger & Puget 1984; Allamandola et al. 1985). Although no specific terrestrial PAH analog was identified as the carrier, such a form of carbonaceous material is likely to produce these bands that are now called PAH features. Interstellar PAHs must enclose $\sim 20\%$ of the overall carbon abundance and must consequently account for a significant fraction of the 2175\AA bump of the extinction curve (see § 4). Due to this large abundance and small size, PAHs must dominate the dust surface and then be a major contributor to the photoelectric heating and to surface reaction (e.g. H_2 formation). On the other hand, the spectrum of the bright PAH features can be used to trace ISM physical conditions and as a probe of star formation activity in the local and distant Universe. PAH has accordingly become an important topic of which a recent review is given by Tielens (2008).

6. Dust Life-Cycle and Evolution

Dust formation has been detected in outflows of AGB stars and in planetary nebulae. Carbon-rich stars mainly produce carbonaceous dust (in some cases SiC) while oxygen rich stars mainly produce silicates. These silicates have a crystallinity up to 15% (Waters 2004) which is higher than for ISM silicates (see § 4). Silicate stardust after being injected into the ISM must then be amorphized, possibly by cosmic ray bombardment (e.g. Demyk et al. 2004). Note that although they can alter it, cosmic rays are not an agent of dust destruction. Dust formation is also observed in supernova ejecta. However, the amount of dust formed in SN that is actually injected into the ISM is controversial since dust destruction also occurs in SN remnants.

Once they are injected into the ISM, dust grains are subjected to many processes that are likely to modify their properties: (i) thermal sputtering by the gas in high-velocity ($> 200 \text{ km s}^{-1}$) shocks; (ii) vaporization and shattering by grain-grain collisions in lower velocity shocks; (iii) alteration/photolysis under cosmic ray or hard photon absorption; and (iv) accretion and coagulation in dense molecular clouds. A description of most of these processes and grain lifetimes in the ISM was presented by Jones (2004).

Dust destruction mainly takes place in the diffuse medium under SN shock wave occurrence. The destruction timescale was estimated to be $\tau_{\text{destruction}} \sim 5 \cdot 10^8 \text{ yrs}$ while considering all possible sources, the dust formation timescale was estimated to be $\tau_{\text{formation}} \sim 3 \cdot 10^9 \text{ yrs}$ (e.g. Jones et al. 1994). A factor of almost 10 between these timescales is inconsistent with the high abundance of dust observed in the ISM. Dust must then be efficiently regenerated in the ISM itself.

Dust has been detected in early Universe objects (quasars, luminous galaxies at $z \sim 6$). The AGB stars whose progenitors are $M_{\star} \sim 1.5 - 3 M_{\odot}$ dominate the dust injection in the disk of mature galaxies. These stars reach the giant branch only after $\sim 700 \text{ Myrs}$ and could then not be responsible for the dust production in the early Universe. On the other hand, in order to explain the dust mass measured in the early Universe SNe should produce $M_{\text{dust}} \gtrsim 1 M_{\odot}/\text{SN}$ (Dwek et al. 2007), a rate that exceeds the observed rate in the local Universe ($M_{\text{dust}} \lesssim 0.02 M_{\odot}/\text{SN}$). This also leads to the conclusion that dust mass must significantly increase in the ISM itself.

Physical conditions in the ISM are not suitable for dust nucleation. However, in the dense ISM (shielded from UV radiation field and SN shock waves), dust can grow by coagulation and by accretion of gas. The timescale for dust “regeneration” by accretion in a dense cloud ($n_{\text{H}} \sim 10^4 \text{ H cm}^{-3}$) is indeed smaller than the cloud life time which is a few million years. Note that the coagulation (of dust grains together) modifies the size distribution but does not increase the total dust mass.

The observed ISM dust grains must have been partially destroyed and regenerated multiple times after their nucleation and must have very different properties compared to “stardusts” (e.g. Zhukovska et al. 2008). Particularly, although nucleated in different stellar environments, silicates and carbonaceous dusts should be mixed by subsequent accretion and coagulation in the ISM. However, this evolutionary scenario seems contradictory with the fact that the bigger silicates and carbonaceous grains are at least partially physically separated in the ISM (see § 4). Although this inconsistency can partly be circumvented by invoking chemically selective accretion processes (see the description by Draine 2009a), it would still hold for the products of coagulation. These

points out the need to know in further detail the processes that drive the dust nucleation and its further evolution and destruction in the ISM.

We note finally that significant dust evolution in the ISM is supported by many pieces of observational evidence. The evolution of the extinction curve (e.g. Fitzpatrick & Massa 1990) mainly traces changes in the size distribution (e.g. Kim et al. 1994). The release (the accretion) of gas species from (onto) the dust can be reflected by variations of the depletion. Such variations are particularly noticeable in SNR where the refractory elements return to the gas phase due to dust destruction (e.g. Slavin 2008). The SED also evolves (e.g. Boulanger et al. 1990; Abergel et al. 2002; Berné et al. 2007) tracing an evolution of the size distribution (e.g. Miville-Deschênes et al. 2002; Stepnik et al. 2003; Compiègne et al. 2008; Flagey et al. 2009) and/or of the physical properties of the emitters (e.g. Berné et al. 2007; Compiègne et al. 2007).

7. Dust Modeling and the DustEM Model

Physical dust models are necessary tools to infer interstellar dust properties from observations. A dust model should ideally satisfy all observable constraints but also make use only of dust components whose presence is plausible in view of likely formation and destruction in the ISM. The history of modern dust models began with Mathis et al. (1977). Like this latter one, early models focused on explaining the extinction (some of them also describing polarization by extinction) using silicates and carbonaceous dust as the grain materials (e.g. Draine & Lee 1984; Kim & Martin 1995). Some models suggested the presence of an organic refractory mantle on the surface of the bigger grains, resulting from the accretion of an ice mantle (H_2O , CH_4 , NH_3) further processed by UV photons (e.g. Greenberg et al. 1995; Li & Greenberg 1997). The Désert et al. (1990) model (hereafter DBP90) was the first that consistently reproduced both extinction and emission, dealing with the stochastic heating mechanism. Most of the current models aim to consistently reproduce the observed extinction and emission (Siebenmorgen & Kruegel 1992; Dwek et al. 1997; Li & Draine 2001; Zubko et al. 2004; Draine & Li 2007, hereafter DL07) as well as the associated polarization (Draine & Fraisse 2009).

Here we focus on the DustEM dust model that is described in Compiègne et al. (2010b). Three dust components are used in this model : (i) PAH, (ii) hydrogenated amorphous carbon (HAC or amC) and (iii) amorphous silicate. PAH optical properties are empirical (described in Li & Draine 2001, and DL07) while the optical efficiencies for the HAC and silicate grains are obtained from the refractive index of bulk material using Mie theory and assuming spherical particles (the simplest approximation). The mass distribution shown in Fig. 5 allows for the reproduction of the observed SED (Fig. 3), extinction curve (Fig. 2) and depletion of the DHGL medium. The observables related to the DHGL medium are commonly used to constrain dust properties and provide a natural reference to compare with when studying dust evolution.

Note that interstellar grains might include components other than hydrocarbons and silicates, for example silicon carbide (SiC), metal oxides (e.g. MgO, FeO), metallic forms of Fe and the minority and trace elements listed in § 3. However, the abundance of such components is sufficiently low to be neglected in models with the current level of sophistication (see also § 2.4 of Draine 2009b).

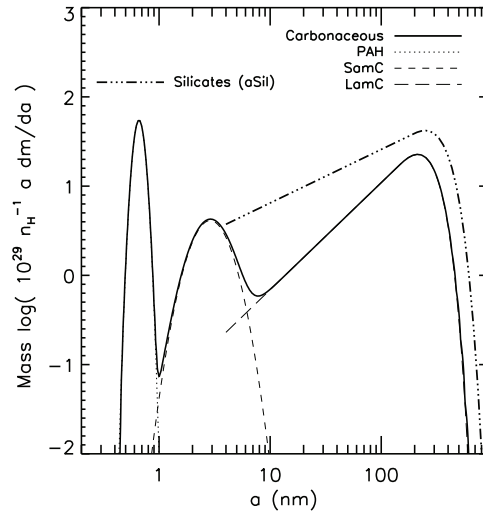


Figure 5. Mass (size) distribution for the dust components used in DustEM model to reproduce the DHGL observables. The population of amorphous carbon dust is split into small (SamC) and large (LamC) grains.

Carbonaceous dust (other than PAH) is often considered to be in the form of crystalline graphite because it can explain the 2175\AA extinction band, but PAH can also account for this band. Moreover, graphite cannot explain the band profile variability observed in the ISM (Fitzpatrick & Massa 2007; Draine 2003). On the other hand, throughout the dust life-cycle, from dense molecular cores to the diffuse ISM, the grain populations are the result of complex, non-equilibrium evolutionary processes and it appears natural to consider that carbon dust is amorphous, as observations have clearly demonstrated for silicate grains. Finally, models show that graphite particles are not efficiently destroyed when encountering a fast shock ($V_S \sim 100 - 150 \text{ km s}^{-1}$) while 80 - 100% of carbon atoms are actually observed to be in the gas phase under such conditions. Conversely, HAC particles seem to be efficiently destroyed. These are the reasons why HAC is used as the carbonaceous grain population in the DustEM DHGL model (see Compiègne et al. 2010b, for the full discussion).

DustEM comprises a SED fitting tool and also allows for the empirical variation of the long wavelength emissivity of dust. Although not presented in Compiègne et al. (2010b), the model deals with the spinning dust millimeter emission and polarization (in extinction and emission). The source code of this model is written in FORTRAN90 and is available online (see Compiègne et al. 2010b).

8. Conclusion

Although the broad lines of dust properties and life-cycle are known, we still lack a detailed understanding: even for the principal dust constituents (silicate and carbonaceous materials) we do not know the exact properties. Furthermore, the carriers of some observables like the DIBs, the ERE, the blue luminescence and the near-IR continuum are poorly or even not identified and are then not included in the general picture of dust models. Details of the efficiency of dust formation, its injection into the ISM, its further

evolution and destruction need to be further investigated. Among the current observing facilities, Herschel and Planck, when combined with Spitzer and IRAS, give access to the entire dust SED (see Fig. 4) and allow us to follow its evolution over a large fraction of the sky (i.e. over a broad range of physical conditions) at scales down to tens of arcseconds. These observations, analyzed with a physical dust model like DustEM (see Abergel et al. 2010; Compiègne et al. 2010a) will certainly provide a new insight into the properties of dust, its evolution and its role in the ISM.

Acknowledgments. I wish to thank the organizers of this conference, especially Roland Kothés and Tom Landecker, for the great job they have done and for the opportunity they offered me to give this review talk.

References

- Abergel, A., et al. 2002, *A&A*, 389, 239
 — 2010, *A&A*, 518, L96+
- Allamandola, L. J., Tielens, A. G. G. M., & Barker, J. R. 1985, *ApJ*, 290, L25
 Allamandola, L. J., Tielens, G. G. M., & Barker, J. R. 1989, *ApJS*, 71, 733
 Asplund, M., Grevesse, N., Sauval, A. J., & Scott, P. 2009, *ARA&A*, 47, 481
 Beelen, A., Cox, P., Benford, D. J., Dowell, C. D., Kovács, A., Bertoldi, F., Omont, A., & Carilli, C. L. 2006, *ApJ*, 642, 694
 Bernard, J., et al. 2010, *A&A*, 518, L88+
- Berné, O., et al. 2007, *A&A*, 469, 575
 Bohlin, R. C., Savage, B. D., & Drake, J. F. 1978, *ApJ*, 224, 132
 Boulanger, F., Abergel, A., Bernard, J.-P., Burton, W. B., Desert, F.-X., Hartmann, D., Lagache, G., & Puget, J.-L. 1996, *A&A*, 312, 256
 Boulanger, F., Cox, P., & Jones, A. P. 2000, in *Infrared Space Astronomy, Today and Tomorrow*, edited by F. Casoli, J. Lequeux, & F. David, 251
 Boulanger, F., Falgarone, E., Puget, J. L., & Helou, G. 1990, *ApJ*, 364, 136
 Boulanger, F., Joblin, C., Jones, A., & Madden, S. (eds.) 2009, *Interstellar Dust from Astronomical Observations to Fundamental Studies*, vol. 35 of EAS Publications Series
- Cardelli, J. A., Meyer, D. M., Jura, M., & Savage, B. D. 1996, *ApJ*, 467, 334
 Compiègne, M., Abergel, A., Verstraete, L., & Habart, E. 2008, *A&A*, 491, 797
 Compiègne, M., Abergel, A., Verstraete, L., Reach, W. T., Habart, E., Smith, J. D., Boulanger, F., & Joblin, C. 2007, *A&A*, 471, 205
 Compiègne, M., Flagey, N., Noriega-Crespo, A., Martin, P. G., Bernard, J. P., Paladini, R., & Molinari, S. 2010a, *ApJL*, submitted
 Compiègne, M., et al. 2010b, *A&A*, submitted
- Dartois, E. 2005, *Space Science Reviews*, 119, 293
 Dartois, E., & Muñoz-Caro, G. M. 2007, *A&A*, 476, 1235
 Demyk, K., d'Hendecourt, L., Leroux, H., Jones, A. P., & Borg, J. 2004, *A&A*, 420, 233
 Désert, F.-X., Boulanger, F., & Puget, J. L. 1990, *A&A*, 237, 215
 Désert, F. X., Boulanger, F., & Shore, S. N. 1986, *A&A*, 160, 295
 Désert, F.-X., et al. 2008, *A&A*, 481, 411
 Dicker, S. R., et al. 2009, *ApJ*, 705, 226
 Draine, B. T. 2003, *ARA&A*, 41, 241
 — 2004, in *The Cold Universe*, Saas-Fee Advanced Course 32, edited by A. W. Blain, F. Combes, B. T. Draine, D. Pfenniger, & Y. Revaz (Springer-Verlag), 213
 — 2009a, in *Cosmic Dust - Near and Far*, edited by T. Henning, E. Grün, & J. Steinacker, vol. 414 of *Astronomical Society of the Pacific Conference Series*, 453
 — 2009b, in *EAS Publications Series*, edited by F. Boulanger, C. Joblin, A. Jones, & S. Madden, vol. 35 of *EAS Publications Series*, 245
 Draine, B. T., & Fraise, A. A. 2009, *ApJ*, 696, 1

- Draine, B. T., & Lee, H. M. 1984, *ApJ*, 285, 89
- Draine, B. T., & Li, A. 2007, *ApJ*, 657, 810
- Draine, B. T., et al. 2007, *ApJ*, 663, 866
- Duley, W. W. 2009, *ApJ*, 705, 446
- Duley, W. W., & Williams, D. A. 1981, *MNRAS*, 196, 269
- Dupac, X., et al. 2001, *ApJ*, 553, 604
- 2003, *A&A*, 404, L11
- Dwek, E. 2005, in *The Spectral Energy Distributions of Gas-Rich Galaxies: Confronting Models with Data*, edited by C. C. Popescu & R. J. Tuffs, vol. 761 of American Institute of Physics Conference Series, 103
- Dwek, E., & Arendt, R. G. 1992, *ARA&A*, 30, 11
- Dwek, E., Galliano, F., & Jones, A. P. 2007, *ApJ*, 662, 927
- Dwek, E., et al. 1997, *ApJ*, 475, 565
- Fitzpatrick, E. L. 1999, *PASP*, 111, 63
- Fitzpatrick, E. L., & Massa, D. 1990, *ApJS*, 72, 163
- 2007, *ApJ*, 663, 320
- Flagey, N., Boulanger, F., Verstraete, L., Miville Deschênes, M. A., Noriega Crespo, A., & Reach, W. T. 2006, *A&A*, 453, 969
- Flagey, N., et al. 2009, *ApJ*, 701, 1450
- Gillett, F. C., Forrest, W. J., & Merrill, K. M. 1973, *ApJ*, 183, 87
- Greenberg, J. M., Li, A., Mendoza-Gomez, C. X., Schutte, W. A., Gerakines, P. A., & de Groot, M. 1995, *ApJ*, 455, L177+
- Henning, T., Grün, E., & Steinacker, J. (eds.) 2009, *Cosmic Dust - Near and Far* (Astronomical Society of the Pacific)
- Jones, A. 2009, in *EAS Publications Series*, edited by F. Boulanger, C. Joblin, A. Jones, & S. Madden, vol. 35 of *EAS Publications Series*, 3
- Jones, A. P. 2000, *J. Geophys. Res.*, 105, 10257
- 2004, in *ASP Conf. Ser. 309: Astrophysics of Dust*, edited by A. N. Witt, G. C. Clayton, & B. T. Draine, 347
- Jones, A. P., Tielens, A. G. G. M., Hollenbach, D. J., & McKee, C. F. 1994, *ApJ*, 433, 797
- Kemper, F., Vriend, W. J., & Tielens, A. G. G. M. 2005, *ApJ*, 633, 534
- Kim, S.-H., & Martin, P. G. 1995, *ApJ*, 444, 293
- Kim, S.-H., Martin, P. G., & Hendry, P. D. 1994, *ApJ*, 422, 164
- Kruegel, E. (ed.) 2003, *The physics of interstellar dust*, *IoP Series in astronomy and astrophysics* (IOP Publishing)
- Léger, A., & Puget, J. L. 1984, *A&A*, 137, L5
- Li, A. 2005, *Journal of Physics Conference Series*, 6, 229
- Li, A., & Draine, B. T. 2001, *ApJ*, 554, 778
- Li, A., & Greenberg, J. M. 1997, *A&A*, 323, 566
- 2003, in *Solid State Astrochemistry*, edited by V. Pirronello, J. Krelowski, & G. Manicò, 37
- Li, M. P., Zhao, G., & Li, A. 2007, *MNRAS*, 382, L26
- Mason, R. E., Wright, G. S., Adamson, A., & Pendleton, Y. 2007, *ApJ*, 656, 798
- Mathis, J. S., Mezger, P. G., & Panagia, N. 1983, *A&A*, 128, 212
- Mathis, J. S., Rumpl, W., & Nordsieck, K. H. 1977, *ApJ*, 217, 425
- Meny, C., Gromov, V., Boudet, N., Bernard, J.-P., Paradis, D., & Nayral, C. 2007, *A&A*, 468, 171
- Meyer, D. M., Jura, M., & Cardelli, J. A. 1998, *ApJ*, 493, 222
- Miville-Deschênes, M., et al. 2010, *A&A*, 518, L104+
- Miville-Deschênes, M.-A., Boulanger, F., Joncas, G., & Falgarone, E. 2002, *A&A*, 381, 209
- Pendleton, Y. J., & Allamandola, L. J. 2002, *ApJS*, 138, 75
- Serkowski, K. 1973, in *IAU Symp. 52: Interstellar Dust and Related Topics*, edited by J. M. Greenberg, & H. C. van de Hulst, 145
- Siebenmorgen, R., & Kruegel, E. 1992, *A&A*, 259, 614
- Slavin, J. 2008, *SSRv*, 143, 311
- Snow, T. P. 2000, *J. Geophys. Res.*, 105, 10239

- Sofia, U. J., & Meyer, D. M. 2001, *ApJ*, 554, L221
- Sofia, U. J., & Parvathi, V. S. 2009, in *Cosmic Dust - Near and Far*, edited by T. Henning, E. Grün, & J. Steinacker, vol. 414 of *ASP Conference Series*, 236
- Stepnik, B., et al. 2003, *A&A*, 398, 551
- Tielens, A. G. G. M. 2008, *ARA&A*, 46, 289
- Trumpler, R. J. 1930, *PASP*, 42, 214
- Wada, S., Mizutani, Y., Narisawa, T., & Tokunaga, A. T. 2009, *ApJ*, 690, 111
- Waters, L. B. F. M. 2004, in *Astrophysics of Dust*, edited by A. N. Witt, G. C. Clayton, & B. T. Draine, vol. 309 of *Astronomical Society of the Pacific Conference Series*, 229
- Weingartner, J. C., & Draine, B. T. 2001, *ApJ*, 548, 296
- Whittet, D. 2003, *Dust in the Galactic environment*, Second Edition (Institute of Physics Publishing)
- Ysard, N., Miville-Deschênes, M. A., & Verstraete, L. 2010, *A&A*, 509, L1+
- Ysard, N., & Verstraete, L. 2010, *A&A*, 509, A12+
- Zhukovska, S., Gail, H.-P., & Trieloff, M. 2008, *A&A*, 479, 453
- Zubko, V., Dwek, E., & Arendt, R. G. 2004, *ApJS*, 152, 211